Downloaded from jnm.snmjournals.org by on March 15, 2017. For personal use only.

^{99m}Tc-Sestamibi Imaging in the Assessment of Toremifene as a Modulator of Multidrug Resistance in Patients with Breast Cancer

Muhammad Mubashar, PhD[1]; Kevin J. Harrington, PhD[2]; Khurram S. Chaudhary, PhD[3]; El-Nasir Lalani, PhD[3]; Gordon W. Stamp, MD[3]; Dudley Sinnett, MD[4]; Daphne M. Glass, DNM[1]; and A. Michael Peters, MD[1]

[1]*Department of Imaging, Hammersmith Hospital, London, United Kingdom;* [2]*Oncology Unit, Imperial Cancer Research Fund, Hammersmith Campus, London, United Kingdom;* [3]*Department of Histopathology, Hammersmith Hospital, London, United Kingdom; and* [4]*Department of Surgery, Charing Cross Hospital, London, United Kingdom*

Multidrug resistance (MDR) due to expression of a membrane-associated permeability glycoprotein (P-glycoprotein [Pgp]) prevents successful cytotoxic chemotherapy for breast cancer. Identification of MDR would facilitate selection of chemotherapy regimens and MDR modulators. This study aimed to evaluate ^{99m}Tc-sestamibi imaging for predicting overexpression of Pgp in primary breast cancer and to measure the efficacy of toremifene, the MDR modulator, in vivo. **Methods:** Twenty patients with untreated breast cancer had ^{99m}Tc-sestamibi imaging 20 and 120 min after tracer injection before and after a 3-d course of toremifene (780 mg/d). Tumor samples were obtained during surgery for correlation of imaging and Pgp immunohistochemistry. **Results:** Sixteen of 20 tumors were visualized with sestamibi. Before toremifene, there was a significant inverse correlation (Spearman rank correlation coefficient [R_S]) between staining intensity, based on the anti-Pgp monoclonal antibodies C494 and C219, and the tumor-to-background ratio (T/B) at 120 min ($R_S = -0.85$; $P < 0.001$ and $R_S = -0.71$; $P < 0.001$, respectively). However, the correlation between the T/B and immunohistochemistry at 20 min was significant only for C494 ($R_S = -0.57$; $P < 0.01$). Similarly, before toremifene, there was an inverse correlation between staining intensity and the change in the T/B between 20 and 120 min ($R_S = -0.77$; $P < 0.001$ and -0.75; $P < 0.001$ for C494 and C219). After toremifene, an inverse correlation between staining intensity and the T/B was seen only at 120 min and only with C494 ($R_S = -0.68$; $P < 0.01$). However, the change in the T/B between 20 and 120 min correlated significantly with staining intensity for C494 and C219 ($R_S = -0.68$; $P < 0.01$ and -0.7; $P < 0.01$ for C494 and C219, respectively). Toremifene did not significantly alter the overall T/B at either 20 or 120 min when data were compared before and after toremifene. Nevertheless, at 120 min, 8 of 8 tumors with low Pgp expression showed reduced uptake after toremifene, whereas 5 of 6 tumors with strong expression showed increased uptake ($P < 0.003$). Moreover, there was a significant correlation between the change in the T/B and staining intensity with C494 ($R_S = 0.59$; $P < 0.05$) and C219 ($R_S = 0.56$; $P < 0.05$) at 120 min but not at 20 min. **Conclusion:** ^{99m}Tc-Sestamibi accumulation in breast cancer correlates with Pgp expression. Toremifene has a dual effect on this accumulation, increasing it through an inhibitory effect on Pgp while at the same time reducing it by a direct competition with sestamibi. The latter implies that in response to Pgp modulation the efflux of various agents may be affected differently.

Key Words: breast cancer; P-glycoprotein; sestamibi; MDR modulation; toremifene

J Nucl Med 2002; 43:519–525

Intrinsic or acquired resistance to cytotoxic chemotherapy represents a major obstacle to the successful treatment of many solid cancers, including breast cancer (*1*). Frequently, cancers exhibit simultaneous cross-resistance to several chemically distinct cytotoxic agents, a phenotype known as multidrug resistance (MDR) (*2,3*). This process involves amplification or overexpression (or both) of specific DNA sequences in drug-resistant, but not drug-sensitive, cells (*4*). The *mdr1* gene on chromosome 7q21-1, which encodes a 170-kDa membrane-associated permeability glycoprotein (P-glycoprotein [Pgp]) (*5*), has been shown to be the chief mediator of the MDR phenotype (*2,3*). Pgp functions as an efflux pump for a diverse range of exogenous (and possibly endogenous) substances, including the anthracyclines (doxorubicin, epirubicin), epipodophyllotoxins (etoposide), vinca alkaloids (vincristine, vinblastine), and taxanes (paclitaxel, docetaxel) (*6*). For a variety of different tumor types, the level of Pgp expression has been shown to correlate with sensitivity to cytotoxic chemotherapy (*7–10*). In addition, Pgp expression has been shown to act as a prognostic factor in patients with breast, lung, gastrointestinal, and gynecologic cancers (*10–17*).

For most patients, the realization that their tumor exhibits the MDR phenotype comes only after chemotherapy has failed to deliver a response. This has the deleterious effects of exposing the patient to the potentially life-threatening side effects of ineffective treatment, delaying instigation of an alternative effective treatment, allowing the tumor to

Received Jul. 16, 2001; revision accepted Nov. 12, 2001.

For correspondence or reprints contact: A. Michael Peters, MD, Department of Nuclear Medicine, Box 170, Addenbrooke's Hospital, Hills Rd., Cambridge, CB2 2QQ, United Kingdom.

E-mail: michael.peters@addenbrookes.nhs.uk

Downloaded from jnm.snmjournals.org by on March 15, 2017. For personal use only.

progress locally or metastasize to distant sites (or both) during the period of ineffective treatment, and enhancing selection of intrinsically aggressive clones by exposing them to sublethal doses of DNA-damaging agents.

Identification of the presence of the MDR phenotype at an early stage, preferably before beginning cytotoxic chemotherapy, would offer the chance of selecting drugs that are known not to be substrates for the Pgp efflux pump (if such agents have proven activity against the specific tumor type) or attempting to decrease the activity of Pgp through the use of specific MDR modulators. Such agents include calcium channel blockers, immunosuppressants, antiestrogens and steroids, antimalarials, calmodulin antagonists, and antithrombotics (*1*). Several of these agents (e.g., verapamil, cyclosporin A, tamoxifen) have significant toxicities at the doses required to modulate MDR in vivo (*18–20*). This fact has limited the clinical application of MDR modulators and provided an impetus to search for novel compounds or analogs of existing compounds with more acceptable toxicity profiles. One such agent is toremifene, a nonsteroidal triphenylethylene antiestrogenic analog of tamoxifen (*21,22*).

Lipophilic ^{99m}Tc-labeled imaging agents, such as sestamibi (hexakis-2-methoxyisobutylisonitrile), that are substrates for Pgp (*23–25*) offer the prospects of scintigraphy to assay functional Pgp status qualitatively and quantitatively in the whole tumor in vivo. In addition, should a tumor be found to be functionally Pgp positive, imaging after administration of MDR-modulating agents would provide a means of measuring the effect of such modulators before using them in conjunction with cytotoxic chemotherapy. Together, such noninvasive imaging protocols would promote rational treatment selection for individual patients on the basis of the functional Pgp status of their tumors. Therefore, to assess these twin goals, ^{99m}Tc-sestamibi imaging was performed on patients with newly diagnosed, primary breast cancer before and after treatment with high doses of the antiestrogenic MDR modulator, toremifene. The levels of ^{99m}Tc-sestamibi tumor accumulation were correlated with the results of immunohistochemical staining for the presence of Pgp.

MATERIALS AND METHODS

Patients

The study was approved by the Local Research Ethics Committee. Patients with palpable, biopsy-proven, treatment-naive, early breast cancer were eligible for inclusion in the study if they were 40–75 y old, with a Karnofsky performance score of >70% and normal hematologic and biochemical parameters. All 20 patients underwent routine preoperative assessment, including hematologic, biochemical, and radiologic (chest radiography and mammography or breast sonography [or both]) examinations and gave written informed consent to participate in the study.

Immunohistochemistry

Tumor samples, obtained at the time of surgical excision, were available for all 20 patients. Immunostaining was performed on 3- to 5-μm formalin-fixed and paraffin-embedded tissue sections using a 3-step immunoperoxidase method. Two murine IgG2a monoclonal antibodies, C219 and C494 (Signet Laboratories, London, Ontario, Canada), which recognize different epitopes on Pgp, were used. In addition, QCRL-1 (Signet Labs.), a murine IgG1 monoclonal antibody that recognizes MDR-related protein (MRP), was used to assess the presence of this mediator of the MDR phenotype. Tissue sections were also stained with the murine monoclonal antibody CK18 (ICRF Laboratories, London, U.K.) as a means of confirming the epithelial origin of tissue samples. Before staining, sections were microwaved (model AVM 902/WH; Philips Whirlpool, Stockholm, Sweden) in citrate buffer to unmask antigenic sites. All primary antibodies were diluted to between 1:10 and 1:40, from an original concentration of approximately 0.1 mg/mL, with phosphate-buffered saline (PBS) containing 0.1% sodium azide and 1% bovine serum albumin and applied to the tissue sections for 2 h at room temperature. Biotinylated rabbit antimouse IgG secondary antibody (Dako A/S, Glostrup, Denmark) was applied for 1 h at room temperature at a dilution of 1:150 in PBS. Horseradish peroxidase–conjugated streptavidin (ID Labs Inc., Glasgow, U.K.) at a dilution of 1:150 was applied as a third layer for 45 min at room temperature and 3,3′-diaminobenzidine (0.25% solution in 0.1% hydrogen peroxide) was added as a chromogen. Sections were counterstained with fresh Cole's hematoxylin (Pioneer Research Chemicals, Colchester, U.K.), dipped in Scott's tap water, immersed briefly in acid alcohol (1% hydrochloric acid/70% ethanol, v/v), dehydrated through sequential alcohol and xylene washes, and mounted using Pertex solution (Cell Path House, Hemel Hempstead, U.K.).

Imaging

Breast imaging was performed after a bolus intravenous injection of 500 MBq ^{99m}Tc-sestamibi (Dupont Pharma, North Billerica, MA) using an MS2 dual-head camera (Siemens, Erlangen, Germany) interfaced to a Macintosh-based computer system. The energy window was set at 15% around the 140-keV photopeak to minimize the effect of scatter. A low-energy, high-resolution collimator was used. The images were acquired using a 256 × 256 matrix at a zoom of 1.6 for the lateral view and 1.23 for the anterior view. The patients were imaged in the following positions: anterior view for immediate dynamic studies, anterior static view for 10 min starting 10 min after injection, and prone lateral static view for 10 min starting 20 min after injection. If the lesion was close to the anterior chest wall, a 30° posterior oblique projection was used. Lead shielding placed between the breasts reduced crosstalk between the breasts. The above static acquisitions were repeated at 2 h after injection of radiotracer.

Toremifene Administration

A ^{99m}Tc-sestamibi study was performed on day 1 before toremifene administration. This was followed by 3 d (days 1–3) of oral treatment with toremifene (Orion Corp., Turku, Finland), 780 mg/d in 3 divided doses. Another ^{99m}Tc-sestamibi study was performed on day 4 within 2 h of the last dose of toremifene. Patients underwent surgical excision of the breast tumor within 24 h of this study. The toxicity of toremifene treatment was assessed by administering a questionnaire at the time the patient underwent the second ^{99m}Tc-sestamibi study.

Data Analysis

Regions of interest (ROIs) were drawn around the tumor and over adjacent background (as a circular line ROI), clearly sepa-

Downloaded from jnm.snmjournals.org by on March 15, 2017. For personal use only.

rated from the tumor ROI. These ROIs, which contained identical pixel numbers before and after toremifene, were copied onto the 2 sets of images by specially designed software that allowed accurate repositioning without disturbance of their relative positions. The accuracy of repositioning of the ROIs was further assessed by comparing their relative positions with heart and liver as internal markers. Counts in the background region were normalized by dividing with the number of pixels in the background region and then multiplying by the tumor areas. Tumor-to-background ratios (T/B) were calculated by dividing the tumor counts by the normalized background counts. The T/B were compared between early and late images in scans before and after toremifene. The T/B for a nonvisualized tumor was assigned a value of 1.

Statistical Analysis

Nonparametric statistics were used. Accordingly, the T/B at individual times after sestamibi injection were expressed as a median and range, whereas the correlations between Pgp expression on immunohistochemical staining and the T/B obtained from ^{99m}Tc-sestamibi imaging were expressed as the Spearman rank correlation coefficient (R_S). Paired data were assessed with the Wilcoxon signed rank test, and proportions were compared using the Fisher exact test. A P of <0.05 that a result could have occurred by chance was regarded as significant.

RESULTS

Immunohistochemistry

All tumor samples showed positive staining with CK18, confirming their epithelial origin. For Pgp staining, tumor samples were examined and scored independently by 2 pathologists who were unaware of the results of the ^{99m}Tc-sestamibi imaging. The following levels of staining intensity for monoclonal antibodies C494 and C219 were defined: complete absence of staining, scored as 0; weakly positive (<5% cells positive), scored as 0.5; tumors with 5%–10% cells positive for Pgp, scored as 1; tumors with >10% cells positive for Pgp, scored as 2; and cells with strong staining, scored as 3. In contrast, all tumor samples were negative for staining with the MRP-specific monoclonal antibody QCRL-1. Representative examples of staining are shown in Figure 1. The results of staining are summarized in Table 1. As can be seen, there was good agreement between the results obtained with C494 and C219.

^{99m}Tc-Sestamibi Imaging Before Toremifene

All 20 patients underwent ^{99m}Tc-sestamibi imaging before toremifene administration according to the described protocol. In 4 patients, the tumor was not visualized at either early or late imaging. The median T/B were 1.79 (range, 1–2.68) and 1.63 (range, 1–2.98) at 20 and 120 min, respectively. For the 16 patients whose tumors were visualized, the T/B increased in 6 and decreased in 10 patients between 20 and 120 min (median, −6.1%; range, −32% to 41%). Representative images are shown in Figure 2. The data for all 20 patients are summarized in Table 1.

The 4 tumors that were not visualized at either 20 or 120 min stained strongly positive for Pgp, all scoring as 3. For all tumors, there was a significant inverse correlation between the staining intensity with C494 and C219 and the 120-min T/B before toremifene, with R_S values of −0.85 ($P < 0.001$) for C494 and −0.71 ($P < 0.001$) for C219. However, the correlation between the T/B and immunohistochemistry at 20 min was significant only for C494 ($R_S = -0.57$; $P < 0.01$). With respect to a change in the T/B between 20 and 120 min, there was a significant inverse correlation with the staining intensity for C494 and C219, with respective R_S values of −0.77 ($n = 16$; $P < 0.001$) and −0.75 ($n = 16$; $P < 0.001$).

^{99m}Tc-Sestamibi Imaging After Toremifene

Seventeen patients underwent imaging after toremifene administration according to the described protocol. Of the patients who did not have further scanning, 1 had diarrhea that was probably attributable to the study medication and 2 withdrew from the study for reasons other than drug toxicity. The overall imaging results were generally altered little by the administration of toremifene (Table 1). Three of the 4 patients whose tumors were not visualized on scintigraphy before toremifene had further imaging and, again, their tumors were not seen. The median T/B after toremifene were 1.71 (range, 1–3.26) and 1.61 (range, 1–2.67) at 20 and 120 min, respectively, neither significantly different from the corresponding values before toremifene. Although the T/B increased in only 1 patient and decreased in 13 patients between 20 and 120 min (median, −13.7%; range,

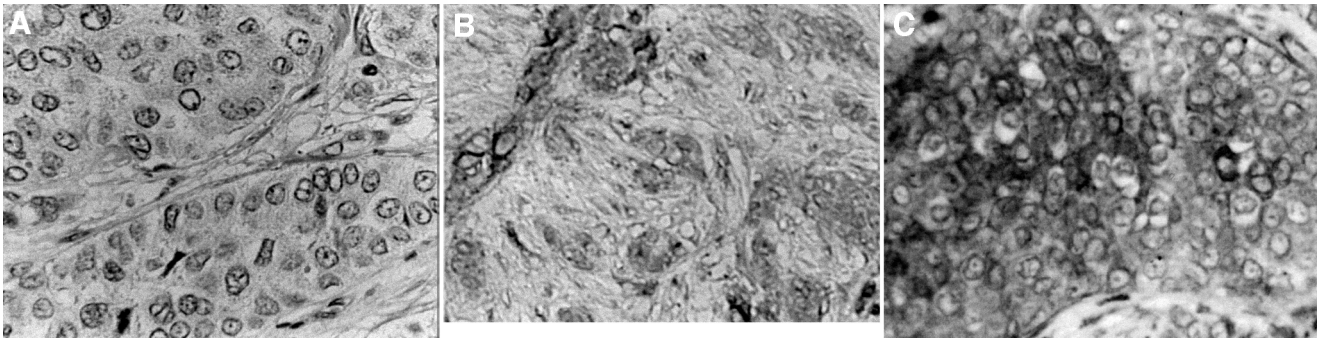

FIGURE 1. Immunohistochemical staining patterns for Pgp in breast cancer. (A) Negative, scored as 0. (B) Positive, scored as 1. (C) Strongly positive, scored as 3.

Downloaded from jnm.snmjournals.org by on March 15, 2017. For personal use only.

TABLE 1
Individual Patient Data

Diagnosis	Size (mm)	T/B* before toremifene		T/B* after toremifene†		Pgp‡	
		20 min	120 min	20 min	120 min	C494	C219
G2 ILC/IDC	30	1.65	1.99	1.35	1.81	0	0
G2 IDC	24	NV	NV	NA	NA	3	3
G1 IDC	20	1.51	1.26	1.52	1.46	2	2
G3 IDC	27	1.76	1.63	1.65	1.36	3	3
G1 IDC	15	1.81	1.89	1.9	1.79	1	0.5
G2 IDC	17	1.84	1.64	1.71	1.61	1	0
G1 IDC	16	NV	NV	NV	NV	3	2
G3 IDC	10	2.2	2.9	3.26	2.67	0	0
G3 IDC	20	1.72	0.64	NA	NA	2	1
G3 IDC	14	NV	NV	NV	NV	3	3
G3 IDC	14	NV	NV	NV	NV	3	2
G3 IDC	25	2.05	1.62	2.17	1.81	3	3
G2 IDC	23	2.24	2.34	2.05	2.04	0	0
G2 IDC	37	2.25	1.52	2.44	1.53	3	3
G2 ILC	45	2.29	1.94	2.58	2.11	2	3
G1 IDC	30	2.68	2.65	2.04	1.99	0	0
G1 IDC	40	2.53	1.99	2.22	1.96	1	1
G2 IDC	15	2.53	2.98	NA	NA	0	0
G3 IDC	25	1.41	1.21	1.52	1.27	2	2
G2 IDC	14	1.23	1.32	1.41	1.19	1	1

*T/B 20 or 120 min after injection of radiotracer.
†Three days after high-dose toremifene treatment.
‡Pgp expression in tumor determined by immunohistochemistry with monoclonal antibodies C494 and C219 (0, no expression; 1, slight expression; 2, moderate expression; 3, strong expression).
G1, G2, G3 = well, moderately, and poorly differentiated, respectively; ILC = intralobular carcinoma; IDC = intraductal carcinoma; NV = not visible; NA = not available.

−37% to 34%), the overall change was not significant compared with that before toremifene ($P > 0.05$; Wilcoxon signed rank test).

After toremifene, a significant inverse correlation between staining intensity and the T/B was seen only at 120 min and only with C494 ($R_S = -0.68$; $n = 17$; $P < 0.01$). However, with respect to a change in the T/B between 20 and 120 min (excluding 3 tumors that were not visualized), there was again a significant inverse correlation with the staining intensity for C494 and C219, with respective R_S values of −0.68 ($n = 14$; $P < 0.01$) and −0.7 ($n = 14$; $P < 0.01$).

Comparison of Data Before and After Toremifene

Although toremifene had no significant effect on the overall T/B at either 20 or 120 min, there were significant positive correlations between the change, induced by toremifene, in the T/B at 120 min and the staining intensities based on C494 ($R_S = 0.59$; $n = 14$; $P < 0.05$) and C219 ($R_S = 0.56$; $n = 14$; $P < 0.05$). With respect to imaging at 20 min, the corresponding correlations did not reach significance (R_S [C219] = 0.46 and R_S [C494] = 0.39; $n = 14$; $P > 0.05$). When patients were classified into those with no staining or weak staining (scores, 0–1) or clear staining (scores 2 and 3), then with either antibody, 8 of 8 patients with low scores showed a decreased T/B at 120 min compared with the value before toremifene at the same time, whereas 5 of 6 patients with high scores showed an increased T/B ($P < 0.003$; Fisher exact test). The picture at 20 min was less clear with corresponding fractions of 5 of 8 and 5 of 6 patients ($P = 0.11$). In other words, in the absence of Pgp, toremifene decreased sestamibi uptake, but this trend was reversed when Pgp was expressed.

Toxicity

Toremifene was generally well tolerated and no serious grade III or grade IV toxicities were recorded. One patient had diarrhea that necessitated withdrawal from the study before further imaging after toremifene. Three patients reported mild nausea and dizziness. In all cases, the side effects resolved completely within 12 h of stopping toremifene administration. All patients were able to undergo surgical tumor resection within 24 h of completing toremifene treatment, and no additional adverse events occurred during the postoperative course that may have been attributable to the drug.

DISCUSSION

Cytotoxic chemotherapy plays a central role in the management of breast cancer. Depending on the clinical situation, there are indications for the use of chemotherapy as

Downloaded from jnm.snmjournals.org by on March 15, 2017. For personal use only.

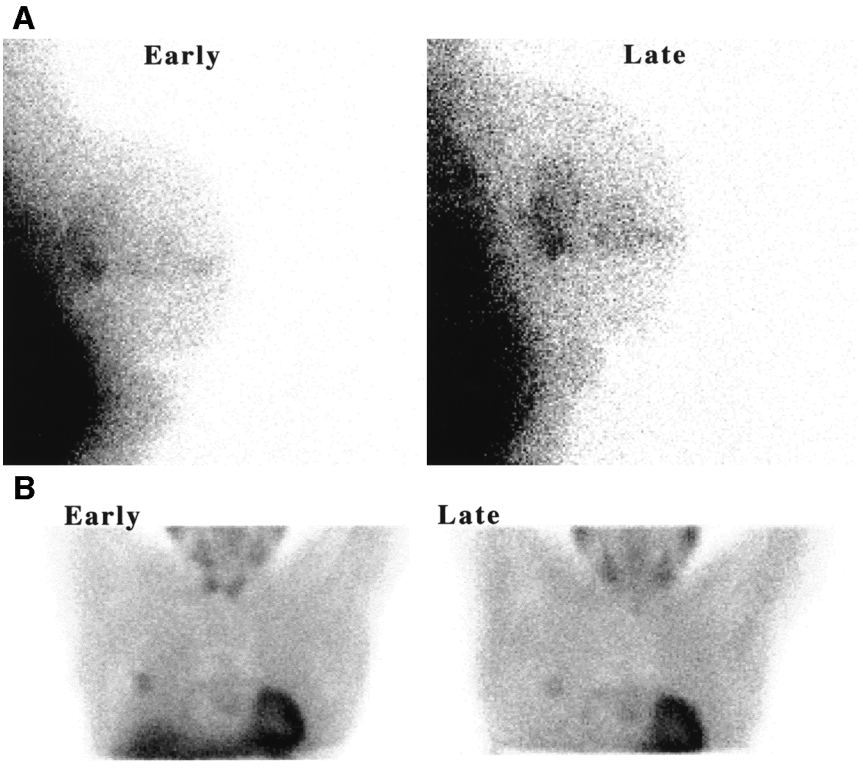

FIGURE 2. ^{99m}Tc-Sestamibi images of breast cancer obtained 20 min (early) and 120 min (late) after injection of radiotracer. (A) Same patient as in Figure 1A with tumor showing T/B that increased from 1.65 to 1.99. (B) Same patient as in Figure 1C with tumor showing T/B that decreased from 2.25 to 1.52.

induction (*26,27*), adjuvant (*28*), and palliative (*29*) treatment. In recent years, there has been increasing interest in the use of induction chemotherapy in patients with breast cancer (*26,27,30*). This approach has several attractions: (a) tumor downstaging in response to chemotherapy may permit breast conservation in cases that would otherwise need radical surgery; (b) the response of the primary tumor predicts the likely chemosensitivity of distant micrometastases; and (c) treatment of subclinical micrometastatic disease commences at the earliest opportunity. Adjuvant chemotherapy has been shown to increase survival in patients with early breast cancer and is widely used (*28*). Palliative chemotherapy can deliver meaningful responses and improve quality of life in patients with metastatic disease but cannot achieve cures (*29*). Anthracyclines, vinca alkaloids, and taxanes are key components of currently prescribed chemotherapy regimens for breast cancer (*26,27,30–32*).

However, in patients with tumors that have an MDR phenotype, existing regimens will not be optimal. The ability to predict this fact before starting chemotherapy might permit selection of an alternative regimen without agents that are Pgp substrates or the additional use of MDR modulators. Thus far, attempts to predict the presence of the MDR phenotype have focused on immunohistochemical staining of tumor biopsies for Pgp protein (*11,12,17,33*) or detection of messenger RNA (mRNA) by the reverse transcriptase polymerase chain reaction (RT-PCR) (*10*). Immunohistochemistry has several potential disadvantages: (a) the patient must undergo a core biopsy; (b) biopsy sampling error may yield false-negative results; (c) Pgp staining patterns may be heterogeneous and so a single histologic assessment may not give an accurate estimate of the degree of drug resistance in the whole tumor; and (d) positive staining for mRNA does not necessarily predict the functional status of Pgp. RT-PCR shares all of the potential sampling problems of immunohistochemistry because only material removed at biopsy is analyzed. In 1 study, RT-PCR detected mRNA for Pgp in 84% of breast tumor samples, most of which were negative for Pgp by immunohistochemistry (*10*), highlighting the potential for false-positive results with this technique. In contrast, ^{99m}Tc-sestamibi imaging can give a global estimate of Pgp function for the whole tumor. In addition, it provides a simple noninvasive means of assessing the effect of putative MDR modulators in vivo.

In these studies, ^{99m}Tc-sestamibi imaging detected 80% of primary breast cancers, which is in line with the findings of previous studies (*34–36*). More important, the results obtained with ^{99m}Tc-sestamibi were shown to correlate with the presence of Pgp expression as assessed by immunohistochemistry. Specifically, the 120-min T/B before and after toremifene were inversely related to the strength of Pgp staining by 2 monoclonal antibodies. However, there was no clearly identified cutoff between the T/B of Pgp-positive and Pgp-negative tumors at either 20 or 120 min. Therefore,

Downloaded from jnm.snmjournals.org by on March 15, 2017. For personal use only.

a single measurement of T/B will predict functional Pgp status in breast tumors with limited reliability. Analysis of the change in T/B between 20 and 120 min (for those tumors in which such an analysis was possible) appeared to be a better predictor of Pgp status. Thus, before toremifene, all 11 tumors that scored 2 or 3 were not visualized or decreased their T/B between 20 and 120 min (100% sensitivity), whereas 6 of 9 tumors with scores of 0–1 increased their T/B (67% specificity). It might be argued that such data have limited clinical usefulness because they add little or nothing to immunohistochemical staining. However, the Pgp staining pattern may not always reflect the functional status of Pgp and the phenotypic presence of MDR. Clearly, further prospective evaluation of ^{99m}Tc-sestamibi imaging, including assessment of subsequent response to chemotherapy, will be required to test this hypothesis.

Significantly, there was evidence that administration of toremifene, given at a dose that has been shown to yield blood levels equivalent to the concentrations required for reversal of MDR in vitro (*22*), altered the results of ^{99m}Tc-sestamibi imaging. Although there were no significant differences between the mean T/B for the scans before and after toremifene at either 20 or 120 min, a significant relationship was found between Pgp positivity and the change in the 120-min T/B induced by toremifene. In addition to the latter findings, toremifene reduced the 120-min T/B in 8 of 8 patients with tumor staining scores of 0–1. The absence of any overall significant change in the T/B can thus be explained by the interaction of 2 opposing effects of toremifene: first, a tendency to modulate Pgp; and, second, interference per se in the accumulation of sestamibi that is unmasked in the absence of Pgp. The mechanism of this latter finding is unclear but may be the result of cellular depolarization that would interfere with the electrostatic trapping of positively charged sestamibi in the negative environment of mitochondria, an effect reported for tamoxifen (*37*). Moreover, this would be consistent with the clearer results obtained with respect to changes in the T/B between 20 and 120 min, or with 120-min data, as opposed to 20-min data, results which suggest that the impact of Pgp, and its modulation by toremifene, is more on retention of substrate than on its initial accumulation.

CONCLUSION

These data suggest that the efflux of various agents may be differentially affected in response to treatment with an MDR modulator and that certain MDR modulators may have properties, in addition to Pgp modulation, that oppose the accumulation of Pgp substrates. Although, in this study, the effect was manifest on a diagnostic radiotracer, it is possible that certain cytotoxic agents might be affected similarly with a resulting reduction in their therapeutic efficacy. Therefore, the finding of a reduction in sestamibi uptake in response to a modulator such as toremifene should identify the likelihood of a limited or unsuccessful response to therapy, whether or not Pgp is suppressed.

REFERENCES

1. Borst P, Pinedo HM. Drug resistance. In: Peckham M, Pinedo HM, Veronesi U, eds. *Oxford Textbook of Oncology*. Oxford, U.K.: Oxford University Press; 1995:586–601.
2. Croop JM, Gros P, Housman DE. Genetics of multidrug resistance. *J Clin Invest.* 1988;81:1303–1309.
3. Bradley G, Ling V. P-glycoprotein, multidrug resistance and tumor progression. *Cancer Metastasis Rev.* 1994;13:223–233.
4. Biedler JL, Riehm H. Cellular resistance to actinomycin D in Chinese hamster cells in vitro: cross-resistance, radioautographic, and cytogenetic studies. *Cancer Res.* 1970;30:1174–1184.
5. Juliano RL, Ling V. A surface glycoprotein modulating drug permeability in Chinese hamster ovary cell mutants. *Biochim Biophys Acta.* 1976;455:152–162.
6. Kaye SB. Multidrug resistance: clinical relevance in solid tumors and strategies for circumvention. *Curr Opin Oncol.* 1998;10(suppl 1):S15–S19.
7. Fojo AT, Shen DW, Mickley LA, Pastan I, Gottesman MM. Intrinsic drug resistance in human kidney cancer is associated with expression of a human multidrug-resistance gene. *J Clin Oncol.* 1987;5:1922–1927.
8. Goldstein LJ, Galski H, Fojo A, et al. Expression of a multidrug resistance gene in human cancers. *J Natl Cancer Inst.* 1989;81:116–124.
9. Goldstein LJ. MDR1 gene expression in solid tumours. *Eur J Cancer.* 1996;32A: 1039–1050.
10. Wang CS, LaRue H, Fortin A, Gariepy G, Tetu B. mdr1 mRNA expression by RT-PCR in patients with primary breast cancer submitted to neoadjuvant therapy. *Breast Cancer Res Treat.* 1997;45:63–74.
11. Verrelle P, Meissonnier F, Fonck Y, et al. Clinical relevance of immunohistochemical detection of multidrug resistance P-glycoprotein in breast carcinoma. *J Natl Cancer Inst.* 1991;83:111–116.
12. Wallner J, Depisch D, Hopfner M, et al. MDR1 gene expression and prognostic factors in primary breast carcinomas. *Eur J Cancer.* 1991;27:1352–1355.
13. Wallner J, Depisch D, Gsur A, Gotzl M, Haider K, Pirker R. MDR1 gene expression and its clinical relevance in primary gastric carcinomas. *Cancer.* 1993;71:667–671.
14. Yamauchi M, Kumazawa H, Satta T, et al. Prediction of doxorubicin resistance in gastrointestinal cancer by P-glycoprotein staining. *Eur J Cancer.* 1992;28A: 1422–1427.
15. Mayer A, Takimoto M, Fritz E, Schellander G, Kofler K, Ludwig H. The prognostic significance of proliferating cell nuclear antigen, epidermal growth factor receptor, and mdr gene expression in colorectal cancer. *Cancer.* 1993;71: 2454–2460.
16. Bourhis J, Goldstein LJ, Riou G, Pastan I, Gottesman MM, Benard J. Expression of a human multidrug resistance gene in ovarian carcinomas. *Cancer Res.* 1989;49:5062–5065.
17. Trock BJ, Leonessa F, Clarke R. Multidrug resistance in breast cancer: a meta-analysis of MDR1/gp170 expression and its possible functional significance. *J Natl Cancer Inst.* 1997;89:917–931.
18. Trump DL, Smith DC, Ellis PG, et al. High-dose oral tamoxifen, a potential multidrug-resistance-reversal agent: phase I trial in combination with vinblastine. *J Natl Cancer Inst.* 1992;84:1811–1816.
19. Weinlander G, Kornek G, Raderer M, Hejna M, Tetzner C, Scheithauer W. Treatment of advanced colorectal cancer with doxorubicin combined with two potential multidrug-resistance-reversing agents: high-dose oral tamoxifen and dexverapamil. *J Cancer Res Clin Oncol.* 1997;123:452–455.
20. Samuels BL, Hollis DR, Rosner GL, et al. Modulation of vinblastine resistance in metastatic renal cell carcinoma with cyclosporine A or tamoxifen: a cancer and leukemia group B study. *Clin Cancer Res.* 1997;3:1977–1984.
21. Kirk J, Houlbrook S, Stuart NS, Stratford IJ, Harris AL, Carmichael J. Selective reversal of vinblastine resistance in multidrug-resistant cell lines by tamoxifen, toremifene and their metabolites. *Eur J Cancer.* 1993;29A:1152–1157.
22. Braybrooke JP, Vallis KA, Houlbrook S, et al. Evaluation of toremifene for reversal of multidrug resistance in renal cell cancer patients treated with vinblastine. *Cancer Chemother Pharmacol.* 2000;46:27–34.
23. Piwnica-Worms D, Chiu ML, Budding M, Kronauge JF, Kramer RA, Croop JM. Functional imaging of multidrug-resistant P-glycoprotein with an organotechnetium complex. *Cancer Res.* 1993;53:977–984.
24. Ballinger JR, Hua HA, Berry BW, Firby P, Boxen I. 99Tcm-Sestamibi as an agent for imaging P-glycoprotein-mediated multi-drug resistance: in vitro and in vivo studies in a rat breast tumour cell line and its doxorubicin-resistant variant. *Nucl Med Commun.* 1995;16:253–257.

Downloaded from jnm.snmjournals.org by on March 15, 2017. For personal use only.

25. Moretti JL, Caglar M, Boaziz C, Caillat-Vigneron N, Morere JF. Sequential functional imaging with technetium-99m hexakis-2-methoxyisobutylisonitrile and indium-111 octreotide: can we predict the response to chemotherapy in small cell lung cancer? *Eur J Nucl Med.* 1995;22:177–180.
26. Fisher B, Brown A, Mamounas E, et al. Effect of preoperative chemotherapy on local-regional disease in women with operable breast cancer: findings from National Surgical Adjuvant Breast and Bowel Project B-18. *J Clin Oncol.* 1997;15:2483–2493.
27. Fisher B, Bryant J, Wolmark N, et al. Effect of preoperative chemotherapy on the outcome of women with operable breast cancer. *J Clin Oncol.* 1998;16:2672–2685.
28. Early Breast Cancer Trialists' Collaborative Group. Systemic treatment of early breast cancer by hormonal, cytotoxic, or immune therapy: 133 randomised trials involving 31,000 recurrences and 24,000 deaths among 75,000 women—Early Breast Cancer Trialists' Collaborative Group. *Lancet.* 1992;339:71–85.
29. Overmoyer BA. Chemotherapeutic palliative approaches in the treatment of breast cancer. *Semin Oncol.* 1995;22(2 suppl 3):2–9.
30. Vlastos G, Mirza NQ, Lenert JT, et al. The feasibility of minimally invasive surgery for stage IIA, IIB, and IIIA breast carcinoma patients after tumor downstaging with induction chemotherapy. *Cancer.* 2000;88:1417–1424.
31. von Minckwitz G, Costa SD, Eiermann W, et al. Maximized reduction of primary breast tumor size using preoperative chemotherapy with doxorubicin and docetaxel. *J Clin Oncol.* 1999;17:1999–2005.
32. Buzdar AU, Singletary SE, Theriault RL, et al. Prospective evaluation of paclitaxel versus combination chemotherapy with fluorouracil, doxorubicin, and cyclophosphamide as neoadjuvant therapy in patients with operable breast cancer. *J Clin Oncol.* 1999;17:3412–3417.
33. Linn SC, Giaccone G, van Diest PJ, et al. Prognostic relevance of P-glycoprotein expression in breast cancer. *Ann Oncol.* 1995;6:679–685.
34. Aktolun C, Bayhan H, Kir M. Clinical experience with Tc-99m MIBI imaging in patients with malignant tumors: preliminary results and comparison with Tl-201. *Clin Nucl Med.* 1992;17:171–176.
35. Khalkhali I, Mena I, Jouanne E, et al. Prone scintimammography in patients with suspicion of carcinoma of the breast. *J Am Coll Surg.* 1994;178:491–497.
36. Palmedo H, Biersack HJ, Lastoria S, et al. Scintimammography with technetium-99m methoxyisobutylisonitrile: results of a prospective European multicentre trial. *Eur J Nucl Med.* 1998;25:375–385.
37. Tuquet C, Dupont J, Mesneau A, Roussaux J. Effects of tamoxifen on the electron transport chain of isolated rat liver mitochondria. *Cell Biol Toxicol.* 2000;16:207–219.

SOCIETY OF NUCLEAR MEDICINE

Downloaded from jnm.snmjournals.org by on March 15, 2017. For personal use only.

The Journal of NUCLEAR MEDICINE

^{99m}Tc-Sestamibi Imaging in the Assessment of Toremifene as a Modulator of Multidrug Resistance in Patients with Breast Cancer

Muhammad Mubashar, Kevin J. Harrington, Khurram S. Chaudhary, El-Nasir Lalani, Gordon W. Stamp, Dudley Sinnett, Daphne M. Glass and A. Michael Peters

J Nucl Med. 2002;43:519-525.

This article and updated information are available at:
http://jnm.snmjournals.org/content/43/4/519

Information about reproducing figures, tables, or other portions of this article can be found online at:
http://jnm.snmjournals.org/site/misc/permission.xhtml

Information about subscriptions to JNM can be found at:
http://jnm.snmjournals.org/site/subscriptions/online.xhtml

The Journal of Nuclear Medicine is published monthly.
SNMMI | Society of Nuclear Medicine and Molecular Imaging
1850 Samuel Morse Drive, Reston, VA 20190.
(Print ISSN: 0161-5505, Online ISSN: 2159-662X)

© Copyright 2002 SNMMI; all rights reserved.

SNMMI SOCIETY OF NUCLEAR MEDICINE AND MOLECULAR IMAGING